Title
Disruption of Transient Serotonin Accumulation by Non-Serotonin-Producing Neurons Impairs Cortical Map Development

Journal
Cell Reports, 10(3)

ISSN
2639-1856

Authors
Chen, Xiaoning
Ye, Ran
Gargus, J Jay
et al.

Publication Date
2015

DOI
10.1016/j.celrep.2014.12.033

Peer reviewed

Article

Cell Reports

Disruption of Transient Serotonin Accumulation by Non-Serotonin-Producing Neurons Impairs Cortical Map Development

Graphical Abstract

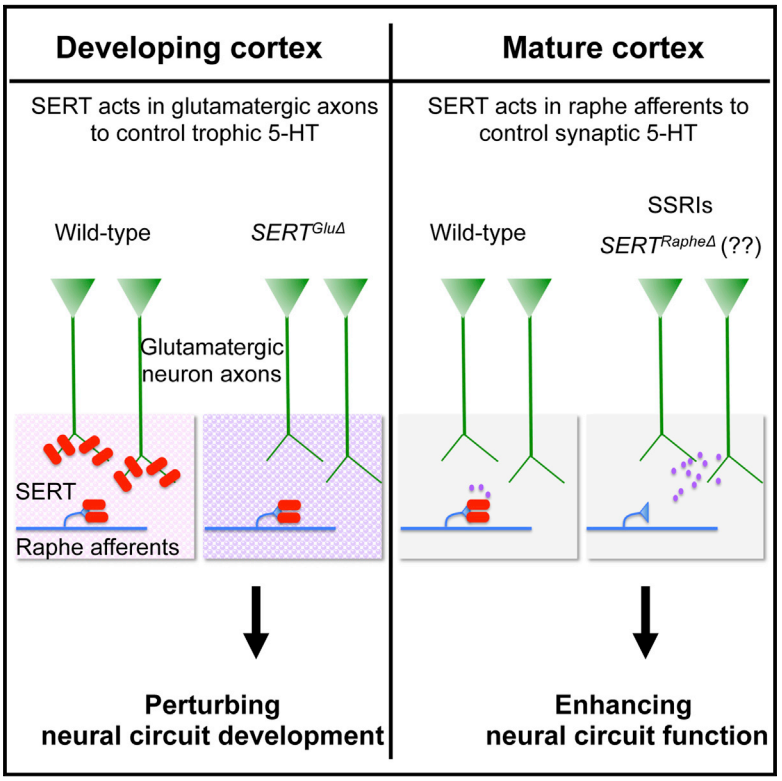

Highlights

- SERT expressed in glutamatergic neuron axons regulates 5-HT in developing CNS
- SERT acts cell autonomously to dictate TCA patterning in sensory cortex
- SERT expressed in TCA shapes spatial organizations of cortical neurons
- Knockout of SERT in TCAs causes excessive 5-HT signals disrupting sensory maps

Authors

Xiaoning Chen, Ran Ye, ..., Kostantin Dobrenis, Ji Ying Sze

Correspondence

jiying.sze@einstein.yu.edu

In Brief

Chen et al. demonstrate that development-specific expression of serotonin transporter SERT in glutamatergic neurons, but not in serotonin-producing neurons, determines morphogenetic serotonin signaling in mouse cortical maturation. This finding provides a mechanistic basis for understanding how SERT-directed drugs produce contrasting effects on neural circuit development compared to adult mental disorder treatments.

Chen et al., 2015, Cell Reports *10*, 346–358
January 20, 2015
http://dx.doi.org/10.1016/j.celrep.2014.12.033

OPEN ACCESS
CellPress

Cell Reports
Article

Disruption of Transient Serotonin Accumulation by Non-Serotonin-Producing Neurons Impairs Cortical Map Development

Xiaoning Chen,[1] Ran Ye,[2] J. Jay Gargus,[3] Randy D. Blakely,[2] Kostantin Dobrenis,[4] and Ji Ying Sze[1,*]
[1]Department of Molecular Pharmacology and Rose F. Kennedy Intellectual and Developmental Disabilities Research Center, Albert Einstein College of Medicine, Bronx, NY 10461, USA
[2]Departments of Pharmacology & Psychiatry, Silvio O. Conte Center for Neuroscience Research, Vanderbilt University, Nashville, TN 37232, USA
[3]Center for Autism Research and Translation and Department of Physiology & Biophysics and Section of Human Genetics in Pediatrics, University of California, Irvine, Irvine, CA 92697, USA
[4]Dominick P. Purpura Department of Neuroscience and Rose F. Kennedy Intellectual and Developmental Disabilities Research Center, Albert Einstein College of Medicine, Bronx, NY 10461, USA
*Correspondence: jiying.sze@einstein.yu.edu
http://dx.doi.org/10.1016/j.celrep.2014.12.033

SUMMARY

Polymorphisms that alter serotonin transporter SERT expression and functionality increase the risks for autism and psychiatric traits. Here, we investigate how SERT controls serotonin signaling in developing CNS in mice. SERT is transiently expressed in specific sets of glutamatergic neurons and uptakes extrasynaptic serotonin during perinatal CNS development. We show that SERT expression in glutamatergic thalamocortical axons (TCAs) dictates sensory map architecture. Knockout of SERT in TCAs causes lasting alterations in TCA patterning, spatial organizations of cortical neurons, and dendritic arborization in sensory cortex. Pharmacological reduction of serotonin synthesis during the first postnatal week rescues sensory maps in *SERT*$^{Glu\Delta}$ mice. Furthermore, knockdown of SERT expression in serotonin-producing neurons does not impair barrel maps. We propose that spatiotemporal SERT expression in non-serotonin-producing neurons represents a determinant in early life genetic programming of cortical circuits. Perturbing this SERT function could be involved in the origin of sensory and cognitive deficits associated with neurodevelopmental disorders.

INTRODUCTION

Dysregulation of serotonin (5-HT) signaling underscores long-standing theories of circuit perturbations that lead to risks for mental disorders. 5-HT acts both as a morphogenetic factor during neural circuit formation and a neuromodulator of circuit plasticity in the mature CNS (Gaspar et al., 2003; Kandel, 2001; Lesch and Waider, 2012). The 5-HT transporter (SERT) controls 5-HT signaling by limiting 5-HT availability to 5-HT receptors (Blakely and Edwards, 2012). Selective 5-HT reuptake inhibitors (SSRIs), which block SERT thus increasing 5-HT signaling, are the first-line treatments for psychiatric traits in adults. However, polymorphisms that reduce SERT gene *Slc6a4* expression/functionality increase the risks for autism and depression and confer abnormal cortical anatomical architecture (Murphy and Lesch, 2008; Pezawas et al., 2005). In rodents, excessive 5-HT triggered by knocking out SERT or the 5-HT degradation enzyme monoamine oxidase A (MAOA) disrupts topographic patterning of the somatosensory barrel and visual cortex and causes anxiety-like behavior (Cases et al., 1996; Murphy and Lesch, 2008; Persico et al., 2001; Upton et al., 2002). Furthermore, administration of SSRIs during the first 2 postnatal weeks was sufficient to confer altered CNS dendritic morphology and increased anxiety-like behavior (Rebello et al., 2014). These observations suggest that SERT exerts distinct biological roles in developing and adult CNS. The mechanism underlying SERT gene function in the developing CNS remains unclear.

Many studies have focused on SERT expressed in brainstem raphe neurons, which constitute the CNS 5-HT-producing neurons and constitutively express SERT at the presynaptic sites along their axons projecting throughout the brain. In the current paradigm, presynaptic SERT reuptakes released 5-HT thereby terminating 5-HT signaling at the synapses (Blakely and Edwards, 2012). This model, however, does not address how SERT controls 5-HT signaling in the developing CNS, where 5-HT is released prior to synapse formation and acts as a trophic factor. In addition, circulating 5-HT of gut, placental, and maternal origins may penetrate into the developing brain (Bonnin and Levitt, 2011). Alternate theories propose that trophic 5-HT is cleared by designated scavenging mechanisms (Vizi et al., 2010). Such mechanism has been explored genetically in *C. elegans*. In *C. elegans*, 5-HT released from 5-HT-producing neurons may travel long distances and be taken up by ectopic neurons (Kullyev et al., 2010). These neurons, referred to as 5-HT-absorbing neurons, use glutamate as the neurotransmitter (Serrano-Saiz et al., 2013) but also express SERT (Jafari et al.,

2011; Ranganathan et al., 2001). By generating transgenic worm lines expressing SERT in specific neurons, we identified that 5-HT-absorbing neurons are essential for preventing excessive 5-HT signals at extrasynaptic targets in a *C. elegans* behavioral circuit (Jafari et al., 2011). These results showed that excessive extrasynaptic 5-HT can perturb neural circuitry and is controlled by SERT gene function in non-5-HT-producing neurons.

5-HT-absorbing neurons were actually first observed in developing brain of mammals including human (Gaspar et al., 2003). Specifically, in rodents between embryonic (E) day 17 and postnatal (P) day 10, SERT is expressed in thalamic neurons that project to sensory cortices, as well as in pyramidal neurons in the prefrontal cortex (PFC) and hippocampus; these neurons also use glutamate as the neurotransmitter while transiently expressing SERT (D'Amato et al., 1987; Hansson et al., 1998; Lebrand et al., 1996, 1998). The timing coincides closely to a period of exuberant synaptogenesis and circuit maturation equivalent to the third trimester of human fetal development. To determine the biological role of 5-HT-absorbing neurons in mammalian brain, we generated transgenic mice with SERT expression knocked out specifically in only 5-HT-absorbing neurons or raphe 5-HT-producing neurons. Using the somatosensory barrel cortex as a model, here we show that SERT expressed in 5-HT-absorbing axons dictates sensory map architectures in the cortex. Our data establish 5-HT-absorbing neurons as essential machinery for controlling 5-HT homeostasis in the developing cortex and suggest that impaired SERT function in 5-HT-absorbing axons could be involved the origin of sensory and cognitive deficits associated with neurodevelopmental disorders.

RESULTS

Selective Knockout of SERT in 5-HT-Producing Neurons or Glutamatergic Thalamic Neurons

To determine if 5-HT-absorbing neurons play a role in mammalian brain, we made use of the exquisite barrel maps located at layer IV of rodent somatosensory cortex. Glutamatergic thalamic ventrobasal (VB) projection neurons convey sensory inputs to the somatosensory cortex, with most of their thalamocortical axons (TCAs) terminating at the receptive fields at layer IV. During the first postnatal week, the TCAs segregate into distinct topographic maps in a sequential order: tangentially oriented TCA terminal arbors corresponding to distinct body parts first segregate into five subfields, and then TCA arbors within each subfield segregate into arrayed patches, with each TCA patch surrounded by a wall of densely packed cortical neurons with their dendrites oriented toward the TCA patch, forming barrel-like structures (Espinosa et al., 2009; Rebsam et al., 2002).

We confirmed SERT mRNA expression in the VB neurons by qPCR and in situ hybridization analysis on P7 mice (Figures 1B and 1C). Using double immunostaining of SERT and the vesicular glutamate transporter 2 (Vglut2), which is predominantly expressed in thalamic and hypothalamic glutamatergic neurons (Fremeau et al., 2001), we observed SERT and Vglut2 coexpressed in TCAs projecting to the somatosensory, visual, and auditory cortex (Figure 2A). In the somatosensory cortex, the temporal evolution of SERT immunoreactivity in the TCAs concurred with barrel development, with the strongest SERT immunoreactivity colocalized with Vglut2$^+$ patches at layer IV (Figures S1 and S2). Vglut2$^+$ TCA SERT immunoreactivity gradually diminished after the first postnatal week and was extinguished by P22 (Figure S1). These results are consistent with prior studies (D'Amato et al., 1987; Lebrand et al., 1998) and show that SERT is expressed in developing Vglut2$^+$ TCAs during the period of barrel formation.

To identify and distinguish the significance of SERT in 5-HT-absorbing axons versus in 5-HT-producing axons, we utilized the Cre/LoxP recombinase system to inactivate SERT expression conditionally (Figure 1A). *SERT$^{fl/fl}$* mice carry LoxP sites flanking exons 3 and 4 of the SERT gene *Slc6a4*. Cre recombinase-mediated deletion results in a reading frameshift designed to eliminate SERT function.

To validate this allele, we crossed *SERT$^{fl/fl}$* into transgenic mice expressing Cre in the germline (*Ella-Cre*). Brain from P7 mice homozygous for this mutation showed no detectable SERT mRNA or immunostaining (Figures 1B, 2A, and 2B). We term this allele *SERT^{Null}*. For all the phenotypes described in this paper, *SERT^{Null}* and the previously existing SERT KO allele (Bengel et al., 1998) conferred comparable effects, and representative results are presented.

To inactivate SERT in TCAs, we utilized *Vglut2-Cre* transgenic mice (Vong et al., 2011). By examining Cre-induced expression of membrane-bound green fluorescence protein (mGFP) and nucleus-targeted β-galactosidase in *Tau$^{mGFP\text{-}nls\text{-}lacZ}$* reporter mice (Hippenmeyer et al., 2005), we identified that *Vglut2-Cre* induced recombination in thalamic neurons but not in raphe neurons (Figures S3A and S3B). By crossing *Vglut2-Cre* into a second reporter mouse strain, *ZsGreen* (Madisen et al., 2010), and performing 5-HT immunostaining, we confirmed the absence of *Vglut2-Cre* activity in raphe 5-HT-producing neurons (Figure S3C). To evaluate *Vglut2-Cre*-mediated SERT deletion, we generated two sets of mice. One set was *SERT$^{fl/fl}$* mice carrying *Vglut2$^{Cre/+}$*(*SERT$^{Glu\Delta}$*) and *SERT$^{fl/fl}$* control littermates. The second set of mice were hybrids designed to reduce concerns over potential nonspecific genetic background effects, generated by crossing *SERT$^{fl/fl}$;Vglut2$^{Cre/+}$* mice with SERT KO mice to obtain *SERT$^{fl/-}$;Vglut2$^{Cre/+}$*(*SERT$^{Glu\Delta/-}$*) mice and control *SERT$^{fl/-}$;Vglut2$^{+/+}$* (*SERT$^{fl/-}$*) littermates. Throughout this paper, comparisons are drawn to littermate mice.

To evaluate *Vglut2-Cre*-induced SERT deletion, we analyzed P7 mice. Both qPCR and in situ hybridization showed dramatically reduced SERT mRNA levels in the VB nuclei of *SERT$^{Glu\Delta}$* mice, whereas their SERT mRNA levels in the brainstem raphe nuclei were comparable to control littermates (Figures 1B and 1C). Double immunostaining of serial tangential sections through the sensory cortices showed no appreciable SERT staining in Vglut2$^+$ TCAs projecting to the sensory cortices in *SERT$^{Glu\Delta}$* and *SERT$^{Glu\Delta/-}$* mice (Figure 2A). In contrast, SERT and 5-HT immunostaining of brainstem sections were comparable between *SERT$^{Glu\Delta}$*, *SERT$^{fl/fl}$*, and WT mice (Figure 2B). Western blots showed that SERT protein abundance in the barrel cortex, but not in the brainstem, was reduced in *SERT$^{Glu\Delta}$* mice (Figure 2C). Combined, these data indicate that *Vglut2-Cre* inactivated SERT expression in the TCAs but did not affect SERT expression in raphe 5-HT-producing neurons.

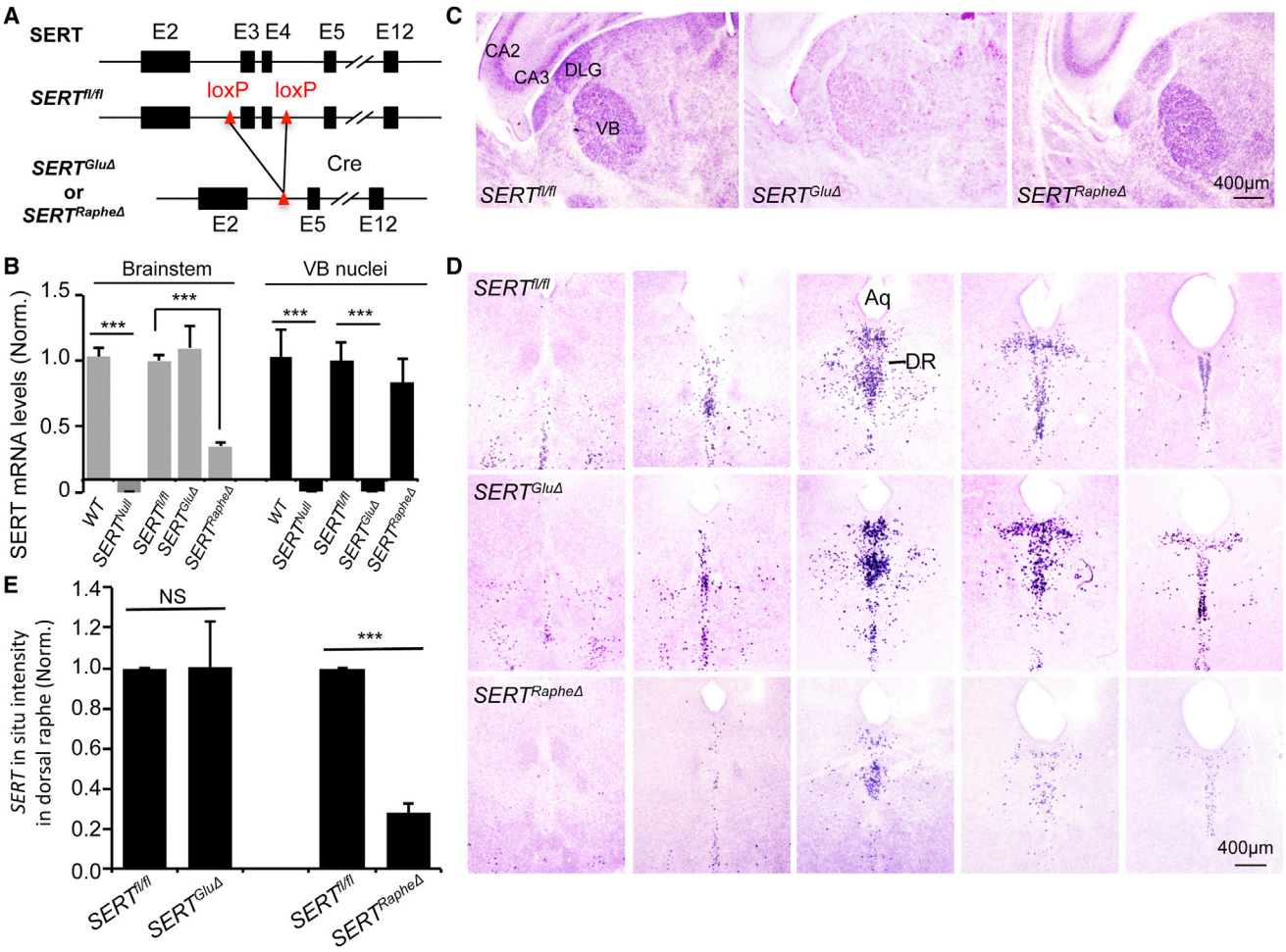

Figure 1. Generation of Transgenic Mice with Selective Knockout of SERT in Vglut2-Expressing Neurons (*SERT*$^{Glu\Delta}$) or Raphe 5-HT-Producing Neurons (*SERT*$^{Raphe\Delta}$)

(A) Schematic illustration of the construction of SERT conditional knockout mice. Two loxP cassettes flank exons 3 and 4 of the SERT gene *Slc6a4*. The reading frame is disrupted when exon 2 splices to exon 5. Rectangles denote exons, and lines denote introns. Transgenic mice carrying the floxed SERT gene (*SERT*$^{fl/fl}$) were crossed with mice expressing Cre in either *Vglut2*$^{+}$ glutamatergic neurons (*SERT*$^{Glu\Delta}$) or *ePet1*$^{+}$ raphe 5-HT-producing neurons (*SERT*$^{Raphe\Delta}$). Transient SERT expression in Vglut2^{+} TCAs projecting to control sensory cortices is shown in Figures S1 and S2, and *Vglut2-Cre*-induced recombination in thalamic neurons is shown in Figure S3.

(B) qPCR analysis of SERT mRNA levels in brainstem and VB nuclei of P7 mice. Results are average of five animals/genotype. Values from *SERT*$^{fl/fl}$ littermates of *SERT*$^{Glu\Delta}$ and *SERT*$^{Raphe\Delta}$ mice were pooled and compared to that of WT, *SERT*$^{Glu\Delta}$, and *SERT*$^{Raphe\Delta}$ mice (mean ± SEM, ***$p < 0.001$, one-way ANOVA).

(C–E) In situ hybridization analysis of SERT mRNA in P7 mice. (C) Representative images showing SERT mRNA expression in thalamic VB and DLG neurons diminished in *SERT*$^{Glu\Delta}$, but not in *SERT*$^{Raphe\Delta}$ mice. Notably, SERT mRNA in hippocampal neurons was also diminished in *SERT*$^{Glu\Delta}$ mice, consistent with *Vglut2-Cre* activity in hippocampal neurons shown in Figure S3. (D) Images of serial coronal sections of brainstem, showing SERT mRNA expression in raphe neurons diminished in *SERT*$^{Raphe\Delta}$, but not in *SERT*$^{Glu\Delta}$ mice. (E) Quantification of SERT^{+} signals in dorsal raphe nuclei (mean ± SEM, ***$p < 0.001$, Student's t test). NS, not significantly different.

To selectively knock out SERT in 5-HT-producing neurons, we utilized *ePet1-Cre* mice, which express Cre in all raphe 5-HT-producing neurons (Scott et al., 2005). qPCR and in situ hybridization showed an ~75% reduction in SERT mRNA levels in the raphe nuclei of P7 *SERT*$^{fl/fl}$;*ePet1*$^{Cre/+}$ (*SERT*$^{Raphe\Delta}$) mice, whereas their SERT mRNA levels in the VB nuclei were unaffected (Figures 1B–1E). Western blots showed a similar reduction of SERT protein abundance in the brainstem of P7 *SERT*$^{Raphe\Delta}$ mice (Figure 2C). Finally, immunostaining of P7 *SERT*$^{Raphe\Delta}$ mice showed substantially reduced SERT abundance in raphe 5-HT-producing neurons, whereas SERT abundance in their Vglut2^{+} TCAs in the sensory cortices was unaffected (Figures 2A and 2B).

Knockout of SERT in Glutamatergic Thalamic Neurons Abolishes 5-HT Uptake by TCAs in Developing Sensory Cortex

To gain insights into the biological role of SERT expressed in 5-HT-absorbing axons and raphe axons, we examined 5-HT immunostaining of P7 somatosensory cortex. In WT and

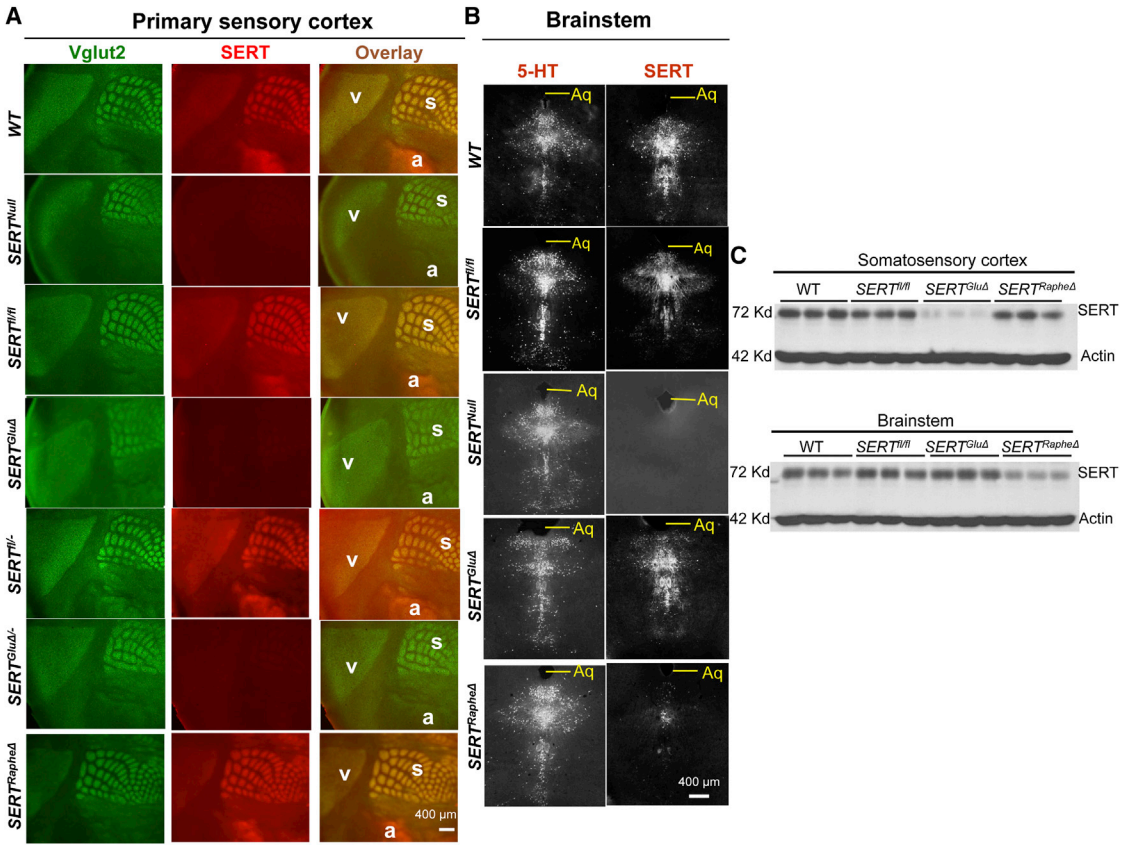

Figure 2. *Vglut2-Cre* Eliminates SERT in TCAs but Not in Raphe Neurons

(A) Vglut2 and SERT double immunolabeling of TCAs projecting to visual (v), auditory (a), and somatosensory barrel (s) cortices on tangential sections of P7 mutant and control littermate mice. SERT staining in the Vglut2$^+$ TCAs was diminished in $SERT^{Glu\Delta}$, $SERT^{Glu\Delta/-}$, and $SERT^{Null}$ but not $SERT^{Raphe\Delta}$ mice. SERT immunohistochemistry on serial tangential sections through the PMBSF from a control mouse is shown in detail in Figure S2.

(B) SERT and 5-HT immunostaining of adjacent coronal sections of the raphe nuclei from P7 mice. SERT staining was abolished in $SERT^{Null}$, diminished in $SERT^{Raphe\Delta}$, but unaffected in $SERT^{Glu\Delta}$ mice. Aq, aqueduct.

(C) Western blots of SERT protein relative to actin in somatosensory barrel cortex and brainstem collected from individual P7 mice. $SERT^{fl/fl}$ mice were littermates of $SERT^{Glu\Delta}$ (one) and $SERT^{Raphe\Delta}$ (two) mice.

$SERT^{fl/fl}$ control mice, immunostaining of 5-HT or SERT on alternate coronal sections of the somatosensory cortex labeled two morphologically distinct types of fibers: fibers that colabeled with Vglut2 immunostaining along the TCAs, and Vglut2-negative fibers that were relatively thicker, highly punctated, and randomly distributed (Figures 3A and S4). In $SERT^{Null}$ mice, there was no appreciable SERT staining, and 5-HT staining of Vglut2$^+$ fibers was abolished. In $SERT^{Raphe\Delta}$ mice, only SERT staining of the thicker fibers was dramatically diminished, suggesting that those fibers represent axons from raphe neurons and release 5-HT. In contrast, in $SERT^{Glu\Delta}$ mice, SERT staining in the thicker 5-HT$^+$ fibers was unaffected, but both 5-HT and SERT staining in Vglut2$^+$ TCAs were diminished (Figures 3A and S4). SERT expression in the raphe neuron afferents explained at least in part for the residual SERT protein observed on the western blots of those P7 $SERT^{Glu\Delta}$ somatosensory cortex samples (Figure 2C). These results indicate that cell-autonomous SERT in Vglut2$^+$ TCAs uptakes 5-HT, and *Vglut2-Cre* abolished this SERT function.

Next, we used high-performance liquid chromatography (HPLC) to measure intracellular 5-HT concentrations in the somatosensory cortex of P7 $SERT^{Glu\Delta}$ and $SERT^{Raphe\Delta}$ mice. We observed a >2-fold reduction in the 5-HT concentration in the somatosensory cortex of P7 $SERT^{Glu\Delta}$ mice compared to control littermates (Figure 3B). In contrast, $SERT^{Raphe\Delta}$ mice did not show a change in the 5-HT concentration in the somatosensory cortex (Figure 3B). The concentrations of norepinephrine and dopamine were not altered in the somatosensory cortex or several other examined brain regions including the brainstem, PFC, and hippocampus in $SERT^{Glu\Delta}$ or $SERT^{Raphe\Delta}$ mice (R.Y. and R.D.B., unpublished data). These results suggest that a large amount of 5-HT in the developing sensory cortex is likely to be trophic 5-HT and is cleared by SERT expressed in the TCAs (Figure 3C).

SERT Expression in TCAs Is Essential for Barrel Map Development

To determine the physiological impact of SERT expressed in TCAs and SERT expressed in raphe axons, we used cytochrome

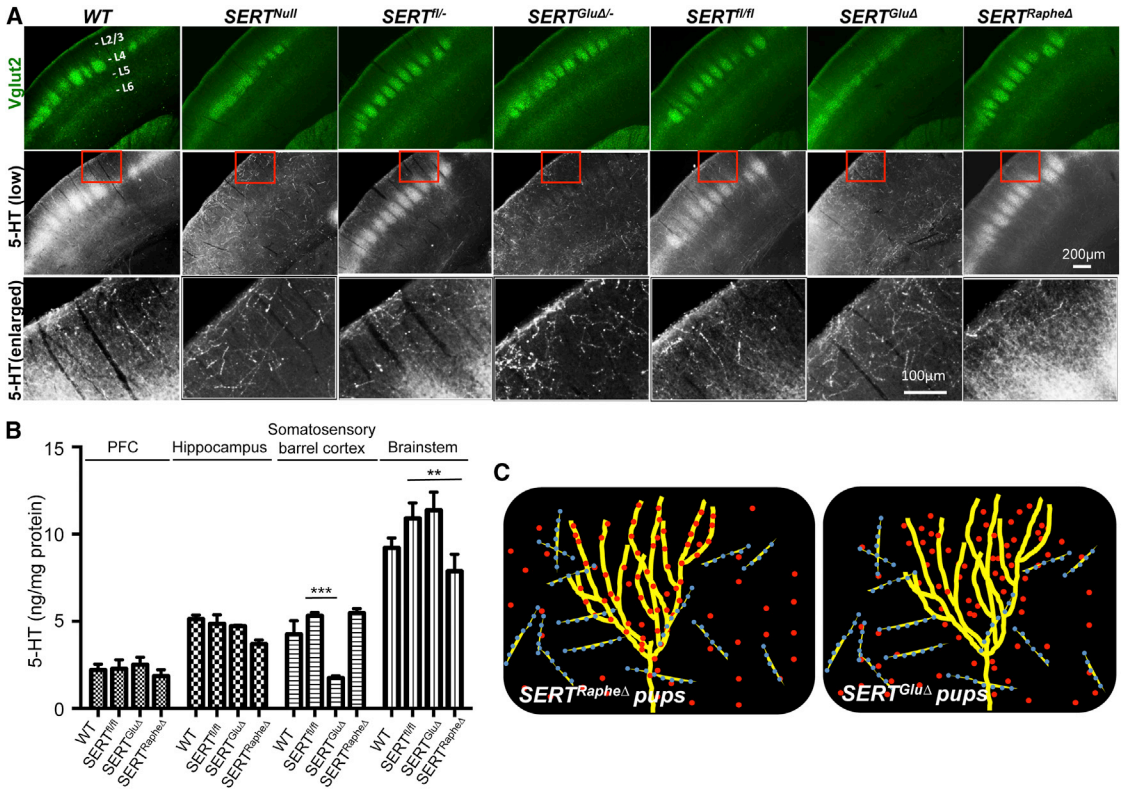

Figure 3. Requirement of SERT Expression in TCAs for 5-HT Uptake in the Barrel Cortex

(A) Double immunohistochemistry for Vglut2 and 5-HT on coronal sections of the somatosensory cortex of P7 mice. The positions of cortical layers are indicated. Third row images show an enlarged view of 5-HT immunohistochemistry in areas outlined by red boxes on images in the second row. Note two types of 5-HT$^+$ fibers in WT and control mice: fibers that colocalized with Vglut2$^+$ TCA patches at layer IV (L4, strongly) and layer VI (L6 weakly), and Vglut2-negative fibers, which were thicker, highly punctated, and randomly distributed. 5-HT staining in Vglut2$^+$ TCAs, not the thicker fibers, was abolished in *SERT*$^{Glu\Delta}$ and *SERT*$^{Glu\Delta/-}$ and *SERT*^{Null} mice. 5-HT staining in Vglut2$^+$ TCAs in *SERT*$^{Raphe\Delta}$ mice was indistinguishable from the control littermate and WT mice. Cortical sections from mutant and control littermate mice were always stained in parallel. For each of the brain samples, alternate sections were analyzed by double immunostaining of Vglut2 and SERT, and data are presented in Figure S4.

(B) HPLC analysis of 5-HT concentrations in brain tissues collected from P7 mice. Values from *SERT*$^{fl/fl}$ littermates of *SERT*$^{Glu\Delta}$ and *SERT*$^{Raphe\Delta}$ mice were pooled and compared to that of WT, *SERT*$^{Glu\Delta}$, and *SERT*$^{Raphe\Delta}$ mice (n = 4, mean ± SEM, **p < 0.01, ***p < 0.001, one-way ANOVA). SERT protein abundance in each of the brain samples was analyzed by western blotting shown in Figure 2C.

(C) Model for SERT expressed in TCAs and raphe afferents during barrel map development: Left, in *SERT*$^{Raphe\Delta}$ mice, TCA-expressed SERT clears 5-HT from the sensory cortex for barrel map development. Right, in *SERT*$^{Glu\Delta}$ mice, trophic 5-HT accumulates around growing TCAs despite SERT expression in raphe afferents and impairs barrel map formation. Yellow lines denote TCAs, blue/yellow lines denote raphe neuron axons, and red dots denote 5-HT.

oxidase (CO) histochemistry to examine barrel patterning in P7 mice. We first confirmed that *SERT*^{Null} disrupts barrel maps. Specifically, in tangential sections through the somatosensory cortex of both SERT KO and *SERT*^{Null} mice, the five sensory subfields at layer IV were intact, but barrels in the subfields corresponding to sinus hairs and paws were largely absent, although barrels in the posteromedial barrel subfield (PMBSF) corresponding to whiskers were preserved (Figures 4A and S5A). This result is consistent with previous studies of the SERT KO mice (Persico et al., 2001) and indicates that the Cre-mediated recombination effectively eliminated SERT gene function.

Because SERT is strongly expressed in raphe neuron axons that arrive at the cortex early during neurogenesis, knockout of SERT in the raphe neurons could severely impair sensory map development. However, *SERT*$^{Raphe\Delta}$ mice developed barrel maps indistinguishable from control littermate and WT mice (Figures 4A and S5A). We next asked whether SERT expressed in TCAs and raphe neuron axons plays a redundant role, thus SERT expression in either TCAs or raphe neuron afferents would be sufficient to direct barrel formation. Against this model, *SERT*$^{Glu\Delta}$ and *SERT*$^{Glu\Delta/-}$ mice displayed disrupted barrel maps akin to SERT KO and *SERT*^{Null} mice as examined at P7 and 6 weeks of age (Figures 4A and S5A). We ruled out disruption of lower sensory relays as a cause for the failure to develop barrel maps, by determining that the architectures of barreloids and barrelettes in the lower sensory stations in the thalamic VB nuclei and brainstem trigeminal nuclei, respectively, were comparable between *SERT*$^{Glu\Delta}$, *SERT*$^{Raphe\Delta}$, their control littermate, and WT mice (Figures S5B and S5C). These data suggest that SERT expressed in the TCAs is essential for establishing sensory maps in the cortex, and this function cannot be compensated by SERT expressed in raphe neuron projections to the cortex.

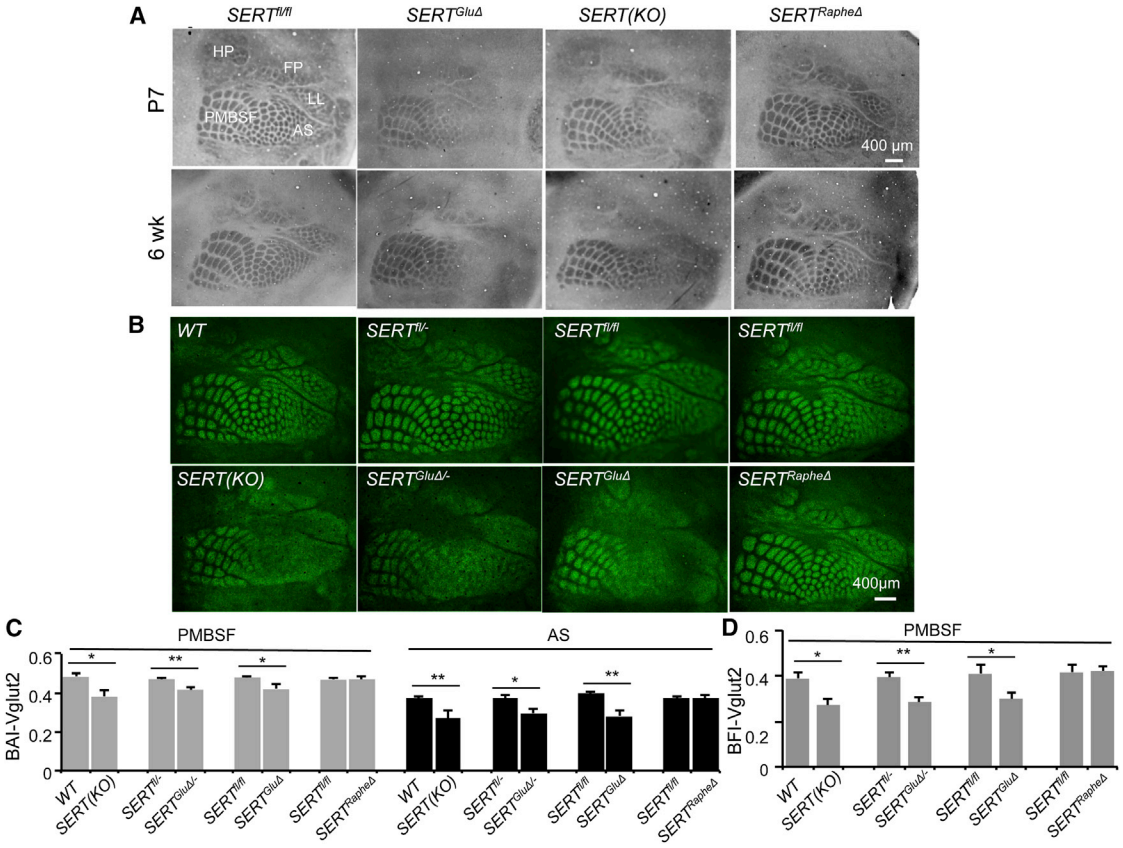

Figure 4. SERT Expressed in TCAs Is Essential for Barrel Map Development

(A) Barrel maps on tangential sections of the somatosensory cortex visualized by CO staining. In $SERT^{Glu\Delta}$ and SERT KO mice, but not in $SERT^{Raphe\Delta}$ mice, barrel structures corresponding to anterior snout (AS), lower lip (LL), forepaw (FP), and hindpaw (HP) were largely absent, but barrels in PMBSF representing whiskers were preserved. Images of CO staining of additional SERT mutant and relative control mice are presented in Figure S5A.

(B) TCA patterning at layer IV visualized by Vglut2 immunostaining of tangential sections through the somatosensory cortex of P7 mice. In $SERT^{Glu\Delta/-}$, $SERT^{Glu\Delta}$, and SERT KO mice, $Vglut2^+$ patches in the PMBSF were discernible but more blurred suggestive of poorer segregation, as compared to corresponding control littermate and WT mice, and $Vglut2^+$ TCA projections to the other barrel subfields failed to display a discernable patterning. Two $SERT^{fl/fl}$ mice each represent control littermates for $SERT^{Glu\Delta}$ and $SERT^{Raphe\Delta}$ mice as shown.

(C and D) Evaluation of $Vglut2^+$ TCA patterning in P7 PMBSF and AS, by calculating BAI-Vglut2 (C) and BFI-Vglut2 (D). Mutant and control littermate mouse samples were stained in parallel (n = 5–6, mean ± SEM, *p < 0.05, **p < 0.01, Student's t test). The differences between WT, $SERT^{Raphe\Delta}$, and control groups and the differences between SERT KO, $SERT^{Glu\Delta}$, and $SERT^{Glu\Delta/-}$ groups were not statistically significant (p = 1, one-way ANOVA followed by Bonferroni test). The methods for quantifying BAI-Vglut2 and BFI-Vglut2 are illustrated in Figure S6.

SERT Expressed in TCAs Governs TCA Terminal Arbor Patterning in the Cortex

The pronounced barrel map defects in $SERT^{Glu\Delta}$ and $SERT^{Glu\Delta/-}$ mice afforded a basis for further investigation into aspects of cyto- and synaptic architectures regulated by SERT function in 5-HT-absorbing axons. The disrupted barrel maps could reflect a requirement of TCA-expressed SERT for TCA segregation. Indeed, Vglut2 immunostaining of P7 mice showed no discernible $Vglut2^+$ TCA patterning in the subfields corresponding to sinus hairs and paws in $SERT^{Glu\Delta}$, $SERT^{Glu\Delta/-}$, SERT KO, and $SERT^{Null}$ mice (Figure 4B). However, in all these SERT mutants, $Vglut2^+$ TCA organization in the PMBSF was largely intact, although the TCA patches were more blurred compared to control littermates (Figure 4B), giving rise to the hypothesis that in the absence of SERT function the TCAs are able to segregate but cannot elaborate a precise patterning.

To test this hypothesis, we evaluated TCA patterning by determining barrel appearance index (BAI) based on Vglut2 immunostaining of TCA patches in the PMBSF and the subfield corresponding to anterior snout (AS) in P7 mice. This procedure provides a quantitative evaluation of the degree to which TCA terminal arbors have compacted into patches reflecting barrel-like organization; more conglobated TCAs become, higher BAI values (Figure S6A) (Toda et al., 2013; Torborg and Feller, 2004). There was no statistical difference in the BAI-Vglut2 values among WT and control groups (p = 1, one-way ANOVA followed by Bonferroni test). In contrast, the BAI-Vglut2 values of both PMBSF and AS were lower in $SERT^{Glu\Delta}$, $SERT^{Glu\Delta/-}$, and SERT KO mice compared to their control littermates and WT mice, indicating defective TCA patterning in both PMBSF and AS in the mutant mice (Figure 4C).

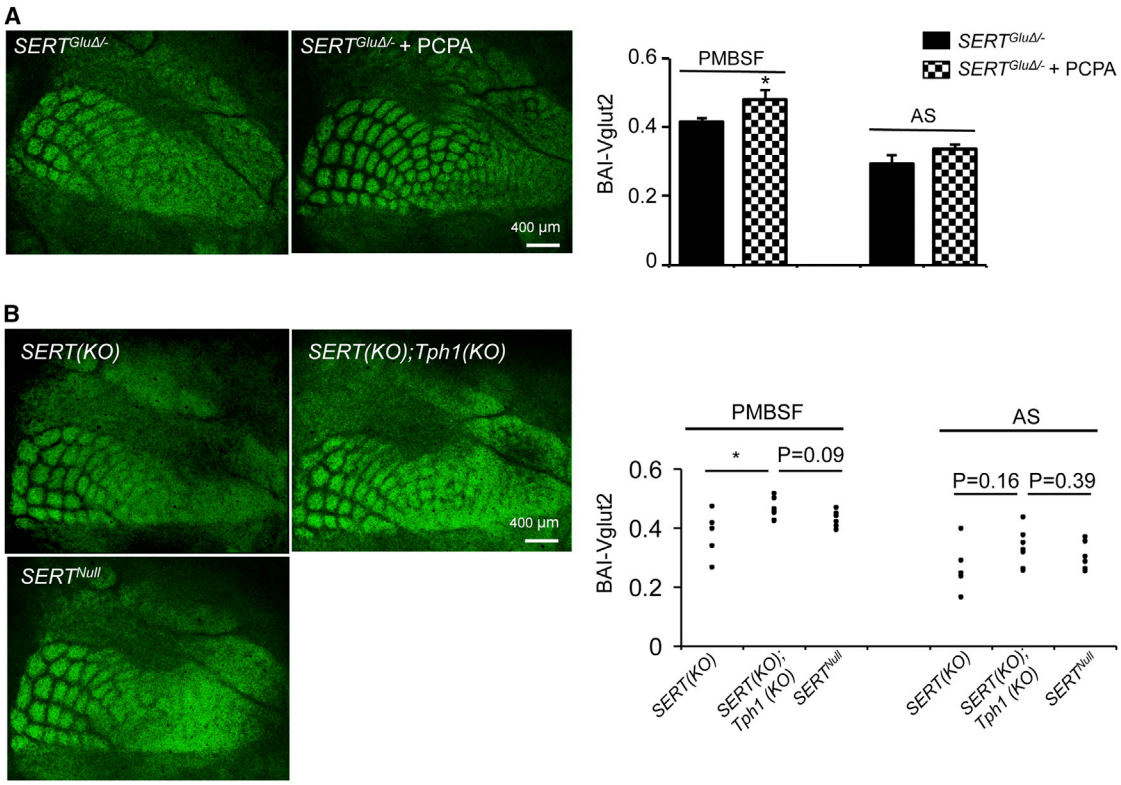

Figure 5. Inhibition of 5-HT Synthesis Rescues TCA Patterning in SERT Mutants

(A) Inhibition of 5-HT synthesis by daily PCPA treatment from P1 to P7 rescued Vglut2^{+} TCA patterning in *SERT*$^{GluΔ/-}$ mice compared to untreated littermates. Daily injection of PCPA at the dosage of 100 mg/kg (n = 6) or 300 mg/kg (n = 4) produced similar effects. Results following 300 mg/kg PCPA treatments are shown (mean ± SEM, *p < 0.05, Student's t test).

(B) Knockout of *Tph1* partially improved Vglut2^{+} TCA patterning in the barrel cortex of SERT KO mice. Each dot represents one mouse (*p < 0.05, Student's t test).

As another method to evaluate TCA architecture, we quantified barrel formation index (BFI), which is a quantitative measure of TCA segregation based on the ratio of Vglut2 immunostaining intensities in barrel hollows to that in the septa region between adjacent barrels (Figure S6B) (Toda et al., 2013). The BFI-Vglut2 values were also significantly lower for *SERT*^{GluΔ}, *SERT*$^{GluΔ/-}$, and SERT KO mice compared to their control mice (Figure 4D). Notably, BAI- and BFI-Vglut2 values among the three SERT mutant groups were not statistically different (p = 1, one-way ANOVA followed by Bonferroni test). Moreover, the same assays indicated that Vglut2^{+} TCA patterning in P7 *SERT*^{RapheΔ} mice was indistinguishable from control littermate and WT mice (Figures 4B–4D). Together, these data support the idea that TCA-expressed SERT underscores a mechanism that defines the precise architecture of TCA patterning in the sensory receptive fields.

Knockout of SERT in TCAs Results in Excessive 5-HT in Developing Cortex

5-HT-absorbing TCAs could serve two possible roles that would distinguish them mechanistically from raphe afferents. First, TCAs might release imported 5-HT at their terminals to guide their terminal arborization, and *SERT*^{GluΔ} reduces the 5-HT signals. We thought this possibility less likely because vesicular monoamine transporter (VMAT)2 KO mice, which cannot release neuronal 5-HT in the brain (Fon et al., 1997; Wang et al., 1997), developed normal barrel maps (Persico et al., 2001; van Kleef et al., 2012). Second, TCA-expressed SERT clears 5-HT from the extracellular space surrounding the developing TCA arbors, creating an environment or guidance cues for the elaboration of TCA patterning. To test this possibility, we treated *SERT*$^{GluΔ/-}$ mice from P1 to P7 with p-chlorophenylalanine (PCPA), an inhibitor of tryptophan hydroxylase, the rate-limiting enzyme for 5-HT synthesis, and examined Vglut2^{+} TCA patterning in the barrel cortex at P7. PCPA treatments rescued barrel maps and increased BAI-Vglut2 values of PMBSF and AS in *SERT*$^{GluΔ/-}$ mice compared to untreated littermates, although the increase in the AS BAI-Vglut2 values was not statistically significant (Figure 5A). These data suggest that disruption of SERT expression in the TCAs results in excessive extracellular 5-HT perturbing TCA patterning.

In addition to 5-HT released from raphe afferents, neonatal brain may contain 5-HT of placental origin or other peripheral sources (Bonnin and Levitt, 2011). We further exploited the role of SERT expressed in 5-HT-absorbing axons, by examining the contribution of nonneuronal 5-HT to TCA patterning. In mammals, placental and peripheral 5-HT synthesis requires the tryptophan hydroxylase encoded by the *Tph1* gene. We

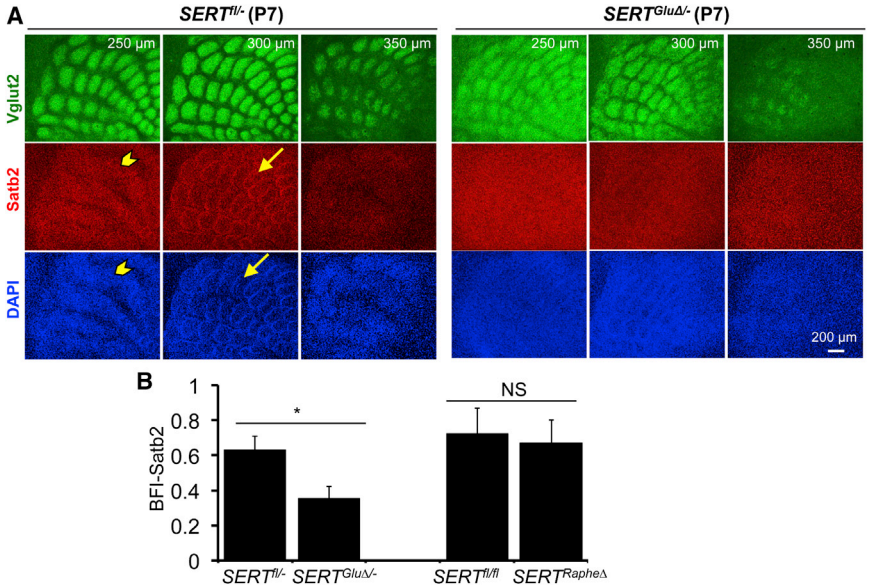

Figure 6. SERT Expressed in TCAs Governs Multiple Spatial Organizations of Satb2$^+$ Neurons in the Somatosensory Cortex

(A) Serial sections through the PMBSF of P7 mice labeled by double immunostaining of Vglut2$^+$ TCAs and Satb2$^+$ cell nuclei, with DAPI counterstain. The distance from the pial surface is indicated. In control littermates (*SERT*$^{fl/-}$), Satb2$^+$ cells, as well as DAPI-labeled nuclei, displayed two distinct patterns: stripes (arrowhead) located ~250 μm from the pial surface and barrels (arrow) located below the stripe structure. Both Satb2$^+$ patterns were largely absent in *SERT*$^{GluΔ/-}$ mice. Impaired spatial organization of other neuronal markers in P7 and mature barrel cortex of *SERT*$^{GluΔ/-}$ mice is shown in Figure S7.

(B) Evaluation of Satb2 barrel structure by calculating BFI of Satb2 immunohistochemistry in P7 PMBSF (n = 5, mean ± SEM, *p < 0.05, Student's t test).

generated SERT;*Tph1* double-knockout mice and compared Vglut2$^+$ TCA patterning in the double mutant with that in SERT KO mice. We observed that Vglut2$^+$ TCA patterning in the barrel cortex was improved, and PMBSF BAI-Vglut2 values were higher in the double-mutant mice compared to SERT KO single-mutant mice, although the increase in AS BAI-Vglut2 values was less pronounced (Figure 5B). There was also a trend of higher BAI-Vglut2 values for the double-mutant mice when compared to *SERT*^{Null} mice (Figure 5B). These data suggest that 5-HT from nonneuronal sources may participate in the developmental processes controlled by TCA-expressed SERT. The relatively modest rescue by inactivating *Tph1* compared to PCPA treatments suggests that the larger potion of 5-HT accumulated in the developing cortex was released by raphe projections. Because *SERT*^{GluΔ} not *SERT*^{RapheΔ} mice displayed defective barrel maps, we conclude that 5-HT signals from neuronal sources in the developing cortex are regulated at least in part by SERT expressed in 5-HT-absorbing axons.

SERT in 5-HT-Absorbing TCAs Specifies Multiple Spatial Organizations of Cortical Neurons

Each barrel is composed of a ring of layer IV cortical neurons forming a wall surrounding a hollow filled with a patch of TCA arbors (for example, see Figure 6A). TCA-expressed SERT could coordinately regulate TCAs and cortical neuron patterning. It remains possible, however, that cortical neuron patterning is predominantly controlled by SERT expressed in raphe projections to the cortex. To discern between the two possibilities, we examined cortical neuron patterning in the PMBSF of *SERT*^{RapheΔ} and *SERT*$^{GluΔ/-}$ mice. We first used the fragile X mental retardation 1 protein (FMRP) as a marker, which is expressed in >97% of layer IV neurons in the barrel cortex (Harlow et al., 2010; Till et al., 2012). Indeed, immunostaining of P7 control mice showed that FMRP$^+$ cells were organized into rings surrounding Vglut2$^+$ TCA patches (Figure S7A). Moreover, we noticed that barrel architectures were not stationary. For example, at 6 weeks of age, Vglut2$^+$ TCA patches were much larger and appeared to be less well segregated, and, interestingly, the ring structure of FMRP$^+$ cells became more prominent (Figure S7A). The FMRP$^+$ cell patterning was impaired in *SERT*$^{GluΔ/-}$ mice at the age of P7 and became almost completely absent in 6 weeks old PMBSF (Figure S7A). To substantiate the observation, we quantified BFI of FMRP immunostaining relative to Vglut2$^+$ TCA patches in the PMBSF. The BFI-FMRP values were significantly lower in *SERT*$^{GluΔ/-}$ mice compared to control littermates both at the age of P7 and 6 weeks old (Figure S7B), showing that disruption of SERT expression in the TCAs impairs the spatial organization of the cortical neurons during the sensory map formation, as well as the trajectory of cortical sensory architectural refinements later in the life.

SERT expressed in the TCAs could influence TCA and cortical neuron patterning in a complementary manner. Namely, as TCA patches elaborate, neurons are instructed to migrate to the space between patches. To further investigate the role of SERT in sensory map formation and to identify which neuronal types are regulated by SERT, and thus 5-HT, we examined cortical neuron patterning using specific cell markers. The transcription factor Satb2 is specifically expressed in excitatory neurons that extend axons across the corpus callosum (Alcamo et al., 2008; Britanova et al., 2008). We were intrigued with the observation made by Killackey and colleagues that callosal projection neurons form temporary barrel structures in the rat somatosensory cortex at the end of postnatal week (Koralek and Killackey, 1990). In keeping with this, immunohistochemistry for Satb2 displayed ring structures surrounding Vglut2$^+$ TCA patches in P7 PMBSF in control mice, very similar to the FMRP immunohistochemistry. The Satb2$^+$ patterning was disrupted in *SERT*$^{GluΔ/-}$ mice (Figure 6). *SERT*^{RapheΔ} mice did not display a detectable Satb2$^+$ patterning defect (Figure 6B), indicating that SERT expressed in 5-HT-absorbing axons is essential for Satb2$^+$ neurons to form the barrel structure.

Moreover, we observed a Satb2$^+$ stripe structure lying on the top of barrels in the PMBSF in control mice; the stripes were also abolished in *SERT*$^{Glu\Delta/-}$ mice (Figure 6A). In addition, rudimental ring structures of DAPI-stained cell nuclei surrounding Vglut2$^+$ TCA patches remained visible in the PMBSF of *SERT*$^{Glu\Delta/-}$, *SERT*$^{Glu\Delta}$, and SERT KO mice (for example, see Figure 6A), indicating that certain layer IV cells were enriched in barrel walls in the absence of SERT function. A simple explanation for these observations would be that TCA-expressed SERT encodes instructions for precise, discrete spatial organizations of specific layer IV neurons in the sensory receptive field, rather than simply driving layer IV neurons to the interbarrel spaces between TCA patches.

SERT Expression in TCAs Shapes Cortical Neuron Dendritic Architecture

As layer IV neurons migrate to barrel walls, they remodel their dendritic architecture by growing dendrites toward the barrel hollow while eliminating unoriented dendritic segments, and this oriented dendrite patterning is thought to serve to sharpen the temporal and spatial precision of the sensory receptive fields (Daw et al., 2007; Espinosa et al., 2009). We assessed *SERT*$^{Glu\Delta}$ and *SERT*$^{Raphe\Delta}$ impact on dendrite patterning, by examining GABAergic dendritic architecture in the barrel cortex. GABAergic neurons constitute ~14% of neurons in the PMBSF, and patterned inhibitory GABA circuits form a scaffold for discriminating local competing sensory inputs (Daw et al., 2007). Immunostaining showed that GABAergic neurons in control mice were arranged into a barrel structure but did not manifest stripes as seen with Satb2$^+$ cells (Figure 7A). *SERT*$^{Raphe\Delta}$ mice displayed a spatial organization of GABA$^+$ cells indistinguishable from control littermates, with an ~2:1 ratio of GABA$^+$ cell densities in barrel walls relative to that in barrel hollows (Figure 7B). In contrast, the PMBSF of *SERT*$^{Glu\Delta/-}$ mice failed to display an appreciable GABA$^+$ cell organization, with nearly an equal GABA$^+$ cell density in barrel walls and hollows (Figures 7A and 7B).

We next characterized GABA dendrite patterning. GABAergic neurons are composed of multiple subpopulations, each expressing distinct molecular markers. To follow particular populations of GABAergic neurons and to enhance the ability to trace complete dendritic trees, we used double immunohistochemistry to identify markers that are expressed in subsets of GABAergic neurons. We found that the calcium-binding protein calretinin is expressed in a small GABA$^+$ population in the barrel cortex (Figure 7C, i and iii). We confirmed calretinin$^+$ processes as dendritic by double immunolabeling with the dendritic marker MAP2. We reconstructed dendritic trees of neurons that were immunolabeled with both GABA and calretinin and located in barrel walls of P7 PMBSF (Figure 7C) and evaluated oriented dendritic arborization based on three parameters: the percentage of total dendrite length, number of dendritic segments, and branchpoints. In *SERT*$^{Raphe\Delta}$ and control PMBSF, calretinin$^+$ GABAergic neurons elaborated their dendrites primarily toward and within a single barrel (Figures 7Cvii and 7D). In contrast, all three parameters showed that calretinin$^+$ GABAergic dendritic segments were not restricted to a primary barrel in *SERT*$^{Glu\Delta}$ and *SERT*$^{Glu\Delta/-}$ PMBSF (Figures 7Cviii and 7D). The differences cannot be attributed to the failure of dendritic development per se because, for example, the total dendrite length and the number of branchpoints did not differ significantly between *SERT*$^{Glu\Delta/-}$ and control littermate mice (218.1 ± 34.5 μm versus 234.3 ± 30.8 μm, p = 0.73, and 4 ± 0.6 versus 5 ± 0.7, p = 0.26, t test, respectively). These data indicate that oriented GABAergic neuron dendritic arborization depends on SERT at work in the TCAs.

DISCUSSION

In this study, we established a biological role for SERT expressed in 5-HT-absorbing axons in developing CNS. We showed that SERT expression in TCAs dictates the spatial organizations of TCA, cortical neurons, and dendrites in the somatosensory cortex. Disruption of SERT expression in the TCAs caused excessive 5-HT leading to permanently impaired sensory architectures. Our data indicate that SERT expressed in 5-HT-absorbing axons is essential machinery for controlling 5-HT signaling in the developing cortex. Because SERT expression in those neurons is transient, our results suggest that regulation of 5-HT signaling in the developing and adult CNS involves distinct SERT mechanisms. SERT is expressed in non-5-HT-producing axons in developing human CNS (Gaspar et al., 2003). It is likely that 5-HT-absorbing axons represent a conserved mechanism regulating trophic 5-HT signals in a period of cortical maturation that lays down the framework of functional neural circuits.

The Role of SERT Expression in 5-HT-Absorbing Axons in Shaping Cortical Architectures

There are at least two mechanisms by which spatiotemporal SERT expression in 5-HT-absorbing axons could control neural patterning. First, 5-HT uptake by TCAs might create a "morphogenic gradient of 5-HT" (Gaspar et al., 2003). This model is conceptually similar to the regulation of pattern formation by classic morphogen gradients (Lander, 2007), predicting that patterned 5-HT signals orchestrate the spatial organizations of the cortex. Another, not necessarily mutually exclusive possibility is that a prompt removal of extracellular 5-HT triggers secondary signals, which, in turn, specify aspects of neural patterning. We found that SERT expression in the TCAs is essential for Satb2$^+$ neurons to form two distinct spatial organizations, barrels, and stripes, in the somatosensory cortex. This observation, combined with the ability of PCPA treatments to rescue the barrel maps in *SERT*$^{Glu\Delta/-}$ mice, points to reducing extracellular 5-HT, rather than 5-HT gradient, as a cue.

Although our data corroborate previous studies of SERT KO and MAOA KO mice indicating that excessive 5-HT impairs barrel formation, 5-HT synthesis and receptor KO mice do not display a prominent pattern defect. This has been interpreted as an indication that the developing brain has other 5-HT sources and redundant 5-HT receptor functions (van Kleef et al., 2012). Our observation that knockout of *Tph1* may partially improve barrel architectures in SERT KO mice indicates that the developing brain is sensitive to nonneuronal 5-HT. However, the modest rescue conferred by eliminating *Tph1* as compared to PCPA treatments implies that a large portion of 5-HT

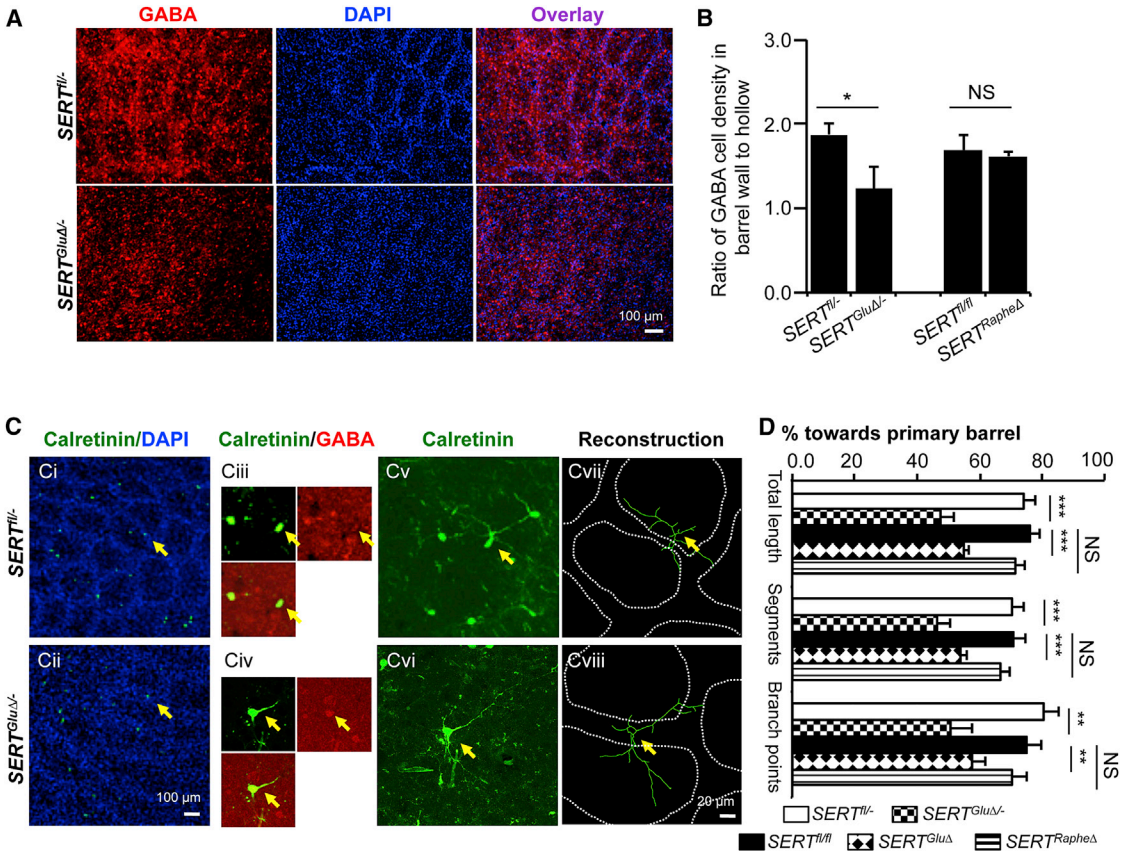

Figure 7. Knockout of SERT Function in TCAs Causes Mistargeting of GABA Dendrites in the Barrel Cortex

(A) Immunohistochemistry for GABA on tangential sections through the PMBSF of P7 mice. In control littermates ($SERT^{fl/-}$), $GABA^+$ cells showed an organization of barrel structures. In the $SERT^{GluΔ/-}$ mice, $GABA^+$ cells failed to form a discernable pattern, even though rudiment ring-like cell arrangements were evident with DAPI counterstain.

(B) Distribution of immunolabeled $GABA^+$ cells in barrel walls delineated by densely packed DAPI-labeled nuclei relative to that in the center of barrel hollows (n = 4–6, mean ± SEM, *$p < 0.05$, Student's t test).

(C) Examples of reconstruction of the dendritic trees of $calretinin^+$ GABAergic neurons located close to the edge of barrel walls in P7 PMBSF. Ci and Cii, low-magnification images show $calretinin^+$ cells (green) at barrel walls delineated by the high density of DAPI-stained nuclei (blue) on tangential sections through the PMBSF. Calretinin immunostaining colocalized with a subset of GABAergic neurons located in the barrel cortex. In three P7 control mice examined, 102 out of 127 $calretinin^+$ neurons at layer IV colabeled with GABA immunostaining. Ciii and Civ representative higher-magnification confocal images show neurons that, labeled with both calretinin (green) and GABA (red), were selected for dendritic reconstruction. Cv and Cvi, higher-magnification confocal images show $calretinin^+$ dendritic profiles. Cvii and Cviii, reconstruction of $calretinin^+$ dendritic trees superimposed over barrel walls from collapsed serial confocal images encompassing 18 μm above and below the center of the cell body. Fourteen to 15 neurons from three mice for each genotype were analyzed.

(D) Selective knockout of SERT in TCAs, not in raphe axons, disrupted oriented $calretinin^+$ GABAergic dendrite patterning. Primary barrels were defined as the barrels that house the majority of total dendritic length (mean ± SEM, **$p < 0.01$, ***$p < 0.001$, Student's t test).

accumulated in the extracellular space is released from raphe projections to the cortex. These observations, together with the requirement of TCA-expressed SERT for barrel map formation, also imply that the developing cortex is, by default, exposed to excess 5-HT, which must be promptly removed in order to form barrel maps. Remarkably, a recent report implicates a sharp drop of extracellular 5-HT levels as a trigger for barrel development (Toda et al., 2013). These findings emphasize that the precise timing of changes in cortical 5-HT-availability is a key to sensory map development. Taken together, it is tempting to speculate that trophic 5-HT signaling inhibits circuit development, and SERT expressed in 5-HT-absorbing axons releases this inhibition, setting the stage for functional circuit formation. In keeping with this hypothesis, elimination of 5-HT1B receptor rescued barrel formation in the complete SERT and MAOA KO models (van Kleef et al., 2012).

In addition to TCAs, SERT is also transiently expressed in pyramidal neurons located in deep layers of the PFC as well as in the hippocampus (Lebrand et al., 1998). Interestingly, selective knockout of SERT expression in those pyramidal neurons by *Emx1-Cre*, which expresses Cre in all cortical and hippocampal excitatory neurons but not in thalamic neurons (Iwasato et al., 2000), did not impair barrel map architecture (X.C. and J.Y.S., unpublished data). Thus, 5-HT-absorbing axons in discrete cortices are likely to control regional trophic 5-HT levels during a precise time window of defined circuit development. Although we have focused on the somatosensory cortex in our studies, our findings could be of general relevance to other cortical

regions that receive innervation of transient 5-HT absorbing axons.

The Role of SERT Expression in 5-HT-Producing Neurons in Sensory Map Development

Despite the intact SERT expression in raphe neuron projections to the sensory cortex in $SERT^{Glu\Delta}$ mice, our data showed that their barrel map defects were comparable to SERT KO and $SERT^{Null}$ mice. Conversely, we have not been able to detect a barrel architectural defect in $SERT^{Raphe\Delta}$ mice. Because *Pet1-Cre* did not completely eliminate SERT expression in the raphe neurons, it is possible that subtle architectural defects in $SERT^{Raphe\Delta}$ mice were not detectable. Nevertheless, the pronounced sensory map defects seen in $SERT^{Glu\Delta}$ mice indicate that SERT function in the raphe axons was insufficient for sensory map development.

In adult CNS, SERT is expressed predominantly, if not exclusively, in raphe 5-HT-producing neurons (Blakely et al., 1991; Hoffman et al., 1991). We propose that the differential SERT expression in the developing versus adult CNS underlies distinct roles of 5-HT signaling. There is abundant evidence that elevated synaptic 5-HT signaling in mature nervous systems facilitates neural circuitry underlying behavior and cognitive function (Kandel, 2001). Defining the precise role of SERT gene function in adult brain, versus its role in development, has been difficult due to the global SERT-null nature of previous models. By uncoupling SERT function in 5-HT-absorbing axons and 5-HT-producing axons, the availability of conditional SERT knockout mice should provide an important opportunity for systematic dissection of how SERT function exerts multiple roles in shaping cortical architecture and circuit function. These animal models may also assist in understanding how SERT antagonists influence both developmental programs as well as the function of mature neural circuitry modulated by 5-HT, and the mechanisms of SERT-directed therapies in the treatment of mental illness.

EXPERIMENTAL PROCEDURES

Animals

Animal procedures were approved by the Albert Einstein College of Medicine Institutional Animal Care and Use Committee. $SERT^{fl/fl}$ mice were generated for our laboratory by Precision Targeting Lab, using homologous recombination of a lox-modified SERT (*Slc6a4*) gene in PTL1 (129B6 hybrid) embryonic stem cells and implanting targeted ES cells into C57BL/6 blastocysts. Two loxP sites were inserted in introns 2 and 4 of *Slc6a4*. The generation of the *Vglut2-Cre*, *ePet1-Cre*, SERT KO, and *Tph1* KO mice has been described previously (Bengel et al., 1998; Scott et al., 2005; Vong et al., 2011; Walther and Bader, 2003). All mouse lines were backcrossed to WT C57BL/6 (Taconic Farms) for at least seven generations. The Cre reporter mouse strains $Tau^{mGFP\text{-}nls\text{-}LacZ}$ (Hippenmeyer et al., 2005) and *Rosa-CAG-LSL-ZsGreen1-WPRE* (*Ai6*) (Madisen et al., 2010) were used for evaluation of *Vglut2-Cre*-induced recombination efficiency.

Quantification of Barrel Map Architecture

The patterning of immunohistochemistry for Vglut2, FMRP, and Satb2 in the somatosensory cortex in various genotypes was evaluated by quantifying barrel formation index (BFI) in the PMBSF, according to a published method (Toda et al., 2013) with modifications. Tangential sections double stained with Vglut2 and FMRP or Satb2 were used for this analysis. Images were processed using the mean filter and band-pass filter tools of ImageJ (NIH) to obtain "smoothened images" (Figure S6B). Fluorescence signal intensities along a rectangular box located in the middle of row C and across C1 to C3 barrels in the smoothed images (red box in Figure S6B) were measured using ImageJ software. We used Vglut2 signals to define barrel structures of C1, C2, and C3 as illustrated in Figure S6B: the horizontal coordinates that had minimal values of Vglut2 signals were defined as representative positions of septa (S), and the distance between two adjacent septa was defined as barrel width (BW). Ten percent of horizontal distance centered on the midpoint of the BW was defined as the center of barrel hollows (H). Vglut2 and Satb2 signal intensities in individual H and S positions were utilized to calculate BFI values. BFI values for Vglut2 (V) were defined by the equation: BFI-Vglut2 = $(V_{H1} + V_{H2} + V_{H3}) / 3 - (V_{S1} + V_{S2} + V_{S3}) / 3)$ / mean intensity of Vglut2 signals in the rectangular box. BFI values for Satb2 (S) were defined by the equation: BFI-Satb2 = $(S_{S1} + S_{S2} + S_{S3}) / 3 - (S_{H1} + S_{H2} + S_{H3}) / 3$ / mean intensity of Satb2 signals in the rectangular box. The same method was used to calculate BFI-FMRP. In this way, BFI values are greater when a neuronal marker is more clearly segregated into barrel structures.

The same original Vglut2 staining images were also used for quantifying overall topography of $Vglut2^+$ TCAs in the PMBSF and the anterior snout-corresponding barrel subfield (AS), by calculating barrel appearance index (BAI), as previously described (Takasaki et al., 2008; Toda et al., 2013). First, the images were processed to determine the threshold values. To do this, a band-pass filter was applied, the minimum values of images were subtracted, the mean value of resulting digital images was determined, and then different threshold values were set as a percentage of the mean values. To determine BAI values, the original images were processed using the rolling ball filter of ImageJ, and the mean values of the images were subtracted. A defined area in the PMBSF and AS was selected as illustrated in Figure S6A, and the total pixels of the selected area and fractions of the pixels with signals higher than the various thresholds within the selected area were obtained by ImageJ. In this paper, BAI values were defined as pixels with fluorescence signals above 30% threshold/total pixels in selected area in PMBSF or AS. BAI values are greater when $Vglut2^+$ TCAs segregated more clearly into individual barrel structures.

SUPPLEMENTAL INFORMATION

Supplemental Information includes Supplemental Experimental Procedures and seven figures and can be found with this article online at http://dx.doi.org/10.1016/j.celrep.2014.12.033.

ACKNOWLEDGMENTS

We thank O. Hobert, G. Schwartz, and C.-W. Chow for helpful discussion and comments; S. Zukin and M. Mehler and their laboratories for reagents and technical help; K. Fisher at the Cellular and Molecular Neuroimaing Core for assistance in GABA dendrite reconstruction and developing methods for quantifying barrel structures; and the Animal Physiology Core for providing brain sectioning equipment. We are grateful to J. Hebert and S. Gokhan for providing Cre reporter mouse lines and M. Gershon for *Tph1* KO mice. We especially thank Dr. B. Lowell for sharing *Vglut2-Cre* transgenic mice prior to the publication. This work was supported by grants from National Institute of Mental Health to J.Y.S. (MH098290 and MH083982) and R.D.B. (MH078028).

Received: January 7, 2014
Revised: November 10, 2014
Accepted: December 15, 2014
Published: January 15, 2015

REFERENCES

Alcamo, E.A., Chirivella, L., Dautzenberg, M., Dobreva, G., Fariñas, I., Grosschedl, R., and McConnell, S.K. (2008). Satb2 regulates callosal projection neuron identity in the developing cerebral cortex. Neuron *57*, 364–377.

Bengel, D., Murphy, D.L., Andrews, A.M., Wichems, C.H., Feltner, D., Heils, A., Mössner, R., Westphal, H., and Lesch, K.P. (1998). Altered brain serotonin homeostasis and locomotor insensitivity to 3, 4-methylenedioxymethamphetamine ("Ecstasy") in serotonin transporter-deficient mice. Mol. Pharmacol. *53*, 649–655.

Blakely, R.D., and Edwards, R.H. (2012). Vesicular and plasma membrane transporters for neurotransmitters. Cold Spring Harb. Perspect. Biol. *4*, 4.

Blakely, R.D., Berson, H.E., Fremeau, R.T., Jr., Caron, M.G., Peek, M.M., Prince, H.K., and Bradley, C.C. (1991). Cloning and expression of a functional serotonin transporter from rat brain. Nature *354*, 66–70.

Bonnin, A., and Levitt, P. (2011). Fetal, maternal, and placental sources of serotonin and new implications for developmental programming of the brain. Neuroscience *197*, 1–7.

Britanova, O., de Juan Romero, C., Cheung, A., Kwan, K.Y., Schwark, M., Gyorgy, A., Vogel, T., Akopov, S., Mitkovski, M., Agoston, D., et al. (2008). Satb2 is a postmitotic determinant for upper-layer neuron specification in the neocortex. Neuron *57*, 378–392.

Cases, O., Vitalis, T., Seif, I., De Maeyer, E., Sotelo, C., and Gaspar, P. (1996). Lack of barrels in the somatosensory cortex of monoamine oxidase A-deficient mice: role of a serotonin excess during the critical period. Neuron *16*, 297–307.

D'Amato, R.J., Blue, M.E., Largent, B.L., Lynch, D.R., Ledbetter, D.J., Molliver, M.E., and Snyder, S.H. (1987). Ontogeny of the serotonergic projection to rat neocortex: transient expression of a dense innervation to primary sensory areas. Proc. Natl. Acad. Sci. USA *84*, 4322–4326.

Daw, M.I., Ashby, M.C., and Isaac, J.T. (2007). Coordinated developmental recruitment of latent fast spiking interneurons in layer IV barrel cortex. Nat. Neurosci. *10*, 453–461.

Espinosa, J.S., Wheeler, D.G., Tsien, R.W., and Luo, L. (2009). Uncoupling dendrite growth and patterning: single-cell knockout analysis of NMDA receptor 2B. Neuron *62*, 205–217.

Fon, E.A., Pothos, E.N., Sun, B.C., Killeen, N., Sulzer, D., and Edwards, R.H. (1997). Vesicular transport regulates monoamine storage and release but is not essential for amphetamine action. Neuron *19*, 1271–1283.

Fremeau, R.T., Jr., Troyer, M.D., Pahner, I., Nygaard, G.O., Tran, C.H., Reimer, R.J., Bellocchio, E.E., Fortin, D., Storm-Mathisen, J., and Edwards, R.H. (2001). The expression of vesicular glutamate transporters defines two classes of excitatory synapse. Neuron *31*, 247–260.

Gaspar, P., Cases, O., and Maroteaux, L. (2003). The developmental role of serotonin: news from mouse molecular genetics. Nat. Rev. Neurosci. *4*, 1002–1012.

Hansson, S.R., Mezey, E., and Hoffman, B.J. (1998). Serotonin transporter messenger RNA in the developing rat brain: early expression in serotonergic neurons and transient expression in non-serotonergic neurons. Neuroscience *83*, 1185–1201.

Harlow, E.G., Till, S.M., Russell, T.A., Wijetunge, L.S., Kind, P., and Contractor, A. (2010). Critical period plasticity is disrupted in the barrel cortex of FMR1 knockout mice. Neuron *65*, 385–398.

Hippenmeyer, S., Vrieseling, E., Sigrist, M., Portmann, T., Laengle, C., Ladle, D.R., and Arber, S. (2005). A developmental switch in the response of DRG neurons to ETS transcription factor signaling. PLoS Biol. *3*, e159.

Hoffman, B.J., Mezey, E., and Brownstein, M.J. (1991). Cloning of a serotonin transporter affected by antidepressants. Science *254*, 579–580.

Iwasato, T., Datwani, A., Wolf, A.M., Nishiyama, H., Taguchi, Y., Tonegawa, S., Knöpfel, T., Erzurumlu, R.S., and Itohara, S. (2000). Cortex-restricted disruption of NMDAR1 impairs neuronal patterns in the barrel cortex. Nature *406*, 726–731.

Jafari, G., Xie, Y., Kullyev, A., Liang, B., and Sze, J.Y. (2011). Regulation of extrasynaptic 5-HT by serotonin reuptake transporter function in 5-HT-absorbing neurons underscores adaptation behavior in Caenorhabditis elegans. J. Neurosci. *31*, 8948–8957.

Kandel, E.R. (2001). The molecular biology of memory storage: a dialogue between genes and synapses. Science *294*, 1030–1038.

Koralek, K.A., and Killackey, H.P. (1990). Callosal projections in rat somatosensory cortex are altered by early removal of afferent input. Proc. Natl. Acad. Sci. USA *87*, 1396–1400.

Kullyev, A., Dempsey, C.M., Miller, S., Kuan, C.J., Hapiak, V.M., Komuniecki, R.W., Griffin, C.T., and Sze, J.Y. (2010). A genetic survey of fluoxetine action on synaptic transmission in Caenorhabditis elegans. Genetics *186*, 929–941.

Lander, A.D. (2007). Morpheus unbound: reimagining the morphogen gradient. Cell *128*, 245–256.

Lebrand, C., Cases, O., Adelbrecht, C., Doye, A., Alvarez, C., El Mestikawy, S., Seif, I., and Gaspar, P. (1996). Transient uptake and storage of serotonin in developing thalamic neurons. Neuron *17*, 823–835.

Lebrand, C., Cases, O., Wehrlé, R., Blakely, R.D., Edwards, R.H., and Gaspar, P. (1998). Transient developmental expression of monoamine transporters in the rodent forebrain. J. Comp. Neurol. *401*, 506–524.

Lesch, K.P., and Waider, J. (2012). Serotonin in the modulation of neural plasticity and networks: implications for neurodevelopmental disorders. Neuron *76*, 175–191.

Madisen, L., Zwingman, T.A., Sunkin, S.M., Oh, S.W., Zariwala, H.A., Gu, H., Ng, L.L., Palmiter, R.D., Hawrylycz, M.J., Jones, A.R., et al. (2010). A robust and high-throughput Cre reporting and characterization system for the whole mouse brain. Nat. Neurosci. *13*, 133–140.

Murphy, D.L., and Lesch, K.P. (2008). Targeting the murine serotonin transporter: insights into human neurobiology. Nat. Rev. Neurosci. *9*, 85–96.

Persico, A.M., Mengual, E., Moessner, R., Hall, F.S., Revay, R.S., Sora, I., Arellano, J., DeFelipe, J., Gimenez-Amaya, J.M., Conciatori, M., et al. (2001). Barrel pattern formation requires serotonin uptake by thalamocortical afferents, and not vesicular monoamine release. J. Neurosci. *21*, 6862–6873.

Pezawas, L., Meyer-Lindenberg, A., Drabant, E.M., Verchinski, B.A., Munoz, K.E., Kolachana, B.S., Egan, M.F., Mattay, V.S., Hariri, A.R., and Weinberger, D.R. (2005). 5-HTTLPR polymorphism impacts human cingulate-amygdala interactions: a genetic susceptibility mechanism for depression. Nat. Neurosci. *8*, 828–834.

Ranganathan, R., Sawin, E.R., Trent, C., and Horvitz, H.R. (2001). Mutations in the Caenorhabditis elegans serotonin reuptake transporter MOD-5 reveal serotonin-dependent and -independent activities of fluoxetine. J. Neurosci. *21*, 5871–5884.

Rebello, T.J., Yu, Q., Goodfellow, N.M., Caffrey Cagliostro, M.K., Teissier, A., Morelli, E., Demireva, E.Y., Chemiakine, A., Rosoklija, G.B., Dwork, A.J., et al. (2014). Postnatal day 2 to 11 constitutes a 5-HT-sensitive period impacting adult mPFC function. J. Neurosci. *34*, 12379–12393.

Rebsam, A., Seif, I., and Gaspar, P. (2002). Refinement of thalamocortical arbors and emergence of barrel domains in the primary somatosensory cortex: a study of normal and monoamine oxidase a knock-out mice. J. Neurosci. *22*, 8541–8552.

Scott, M.M., Wylie, C.J., Lerch, J.K., Murphy, R., Lobur, K., Herlitze, S., Jiang, W., Conlon, R.A., Strowbridge, B.W., and Deneris, E.S. (2005). A genetic approach to access serotonin neurons for in vivo and in vitro studies. Proc. Natl. Acad. Sci. USA *102*, 16472–16477.

Serrano-Saiz, E., Poole, R.J., Felton, T., Zhang, F., De La Cruz, E.D., and Hobert, O. (2013). Modular control of glutamatergic neuronal identity in C. elegans by distinct homeodomain proteins. Cell *155*, 659–673.

Takasaki, C., Okada, R., Mitani, A., Fukaya, M., Yamasaki, M., Fujihara, Y., Shirakawa, T., Tanaka, K., and Watanabe, M. (2008). Glutamate transporters regulate lesion-induced plasticity in the developing somatosensory cortex. J. Neurosci. *28*, 4995–5006.

Till, S.M., Wijetunge, L.S., Seidel, V.G., Harlow, E., Wright, A.K., Bagni, C., Contractor, A., Gillingwater, T.H., and Kind, P.C. (2012). Altered maturation of the primary somatosensory cortex in a mouse model of fragile X syndrome. Hum. Mol. Genet. *21*, 2143–2156.

Toda, T., Homma, D., Tokuoka, H., Hayakawa, I., Sugimoto, Y., Ichinose, H., and Kawasaki, H. (2013). Birth regulates the initiation of sensory map formation through serotonin signaling. Dev. Cell *27*, 32–46.

Torborg, C.L., and Feller, M.B. (2004). Unbiased analysis of bulk axonal segregation patterns. J. Neurosci. Methods *135*, 17–26.

Upton, A.L., Ravary, A., Salichon, N., Moessner, R., Lesch, K.P., Hen, R., Seif, I., and Gaspar, P. (2002). Lack of 5-HT(1B) receptor and of serotonin transporter have different effects on the segregation of retinal axons in the lateral geniculate nucleus compared to the superior colliculus. Neuroscience *111*, 597–610.

van Kleef, E.S., Gaspar, P., and Bonnin, A. (2012). Insights into the complex influence of 5-HT signaling on thalamocortical axonal system development. Eur. J. Neurosci. *35*, 1563–1572.

Veenstra-VanderWeele, J., Muller, C.L., Iwamoto, H., Sauer, J.E., Owens, W.A., Shah, C.R., Cohen, J., Mannangatti, P., Jessen, T., Thompson, B.J., et al. (2012). Autism gene variant causes hyperserotonemia, serotonin receptor hypersensitivity, social impairment and repetitive behavior. Proc. Natl. Acad. Sci. USA *109*, 5469–5474.

Vizi, E.S., Fekete, A., Karoly, R., and Mike, A. (2010). Non-synaptic receptors and transporters involved in brain functions and targets of drug treatment. Br. J. Pharmacol. *160*, 785–809.

Vong, L., Ye, C., Yang, Z., Choi, B., Chua, S., Jr., and Lowell, B.B. (2011). Leptin action on GABAergic neurons prevents obesity and reduces inhibitory tone to POMC neurons. Neuron *71*, 142–154.

Walther, D.J., and Bader, M. (2003). A unique central tryptophan hydroxylase isoform. Biochem. Pharmacol. *66*, 1673–1680.

Wang, Y.M., Gainetdinov, R.R., Fumagalli, F., Xu, F., Jones, S.R., Bock, C.B., Miller, G.W., Wightman, R.M., and Caron, M.G. (1997). Knockout of the vesicular monoamine transporter 2 gene results in neonatal death and supersensitivity to cocaine and amphetamine. Neuron *19*, 1285–1296.